

Narrowing the filter cavity bandwidth via optomechanical interaction

Yiqiu Ma,^{1,*} S. L. Danilishin,¹ Chunnong Zhao,^{1,†} Haixing Miao,^{2,‡}
W. Z. Korth,^{2,3} Yanbei Chen,³ Robert Ward,⁴ and D. G. Blair¹

¹*School of Physics, University of Western Australia, WA 6009, Australia*

²*LIGO Laboratory, California Institute of Technology, Pasadena, California 91125 USA*

³*Theoretical Astrophysics 350-17, California Institute of Technology, Pasadena, CA 91125, USA*

⁴*Center for Gravitational Physics, Department of Quantum Science,
Australian National University, Canberra ACT 0200 Australia*

We propose using optomechanical interaction to narrow the bandwidth of filter cavities for achieving frequency-dependent squeezing in advanced gravitational-wave detectors, inspired by the idea of optomechanically induced transparency. This not only allows us to achieve narrow bandwidth, comparable to the detection band of few hundred Hz, with tabletop optical cavities, but also to tune the bandwidth over a wide range, which is ideal for optimizing sensitivity for different gravitational-wave sources. The experimental challenge for its implementation is the stringent requirement on low thermal noise, which would need superb mechanical quality factor that is quite difficult to achieve by using currently-available low-loss mechanical oscillators; one possible solution is to use optical dilution of the mechanical damping, which can considerably relax the requirement on the mechanics.

PACS numbers:

Introduction.— Advanced interferometric gravitational wave detectors, e.g., the Advanced LIGO [1], are expected to be limited in sensitivity by noise of quantum origin over most of the detection band. Further enhancement of these quantum-limited detectors requires manipulation of the optical field and the readout scheme at a quantum level such that the quantum noise is reduced over the entire detection band. One approach suggested by Kimble *et al.* [2] is to inject frequency-dependent squeezed light into the interferometer, using a cascade of optical cavities to rotate the squeezing angle in a frequency-dependent way. The filter cavity bandwidth needs to be of the order of 100Hz. The scheme proposed is using relatively low-finesse cavities of kilometer scale, comparable to the size of the interferometer, an ambitious and costly plan. If one instead would like to use a short filter cavity, e.g, of the order of few meters or less on a tabletop, this implies a cavity finesse around 10^6 . At this finesse, even small optical losses will destroy the quantum coherence of the squeezed light. Recently, a design using 2-mirror linear cavity proposed by Evans *et al.* [3] opens the possibility to overcome this problem, using cavities on the orders of ten meters. Another proposed solution is to actively narrow the cavity bandwidth by taking the advantage of the narrow-band dispersion created by electromagnetic induced transparency (EIT) in atomic system [4], which effectively slows the light and increases the cavity storage time. However, a typical atomic setup is generally quite lossy and the narrow-band dispersion is accompanied by a strong absorption. Not only is the loss an issue, but also what we need here is an all-pass filter (ideally), only changing the phase of the squeezed light.

Motivated by the idea of optomechanically induced transparency (OMIT), which has recently been experi-

mentally demonstrated by Weis *et al.* [5] and Teufel *et al.* [6], here we propose to narrow the filter cavity bandwidth via optomechanical interaction. As illustrated in Fig.1, the filter cavity consists of a mirror-endowed mechanical oscillator with eigenfrequency ω_m that is much larger than the cavity bandwidth γ . A control laser drives the filter cavity at frequency ω_p , detuned from the cavity resonant frequency ω_0 (also the laser frequency of the main interferometer) by $\omega_m - \delta$ with δ comparable to the gravitational-wave signal frequency Ω . As we will show, the optomechanical interaction modifies the cavity response and gives rise to the following input-output

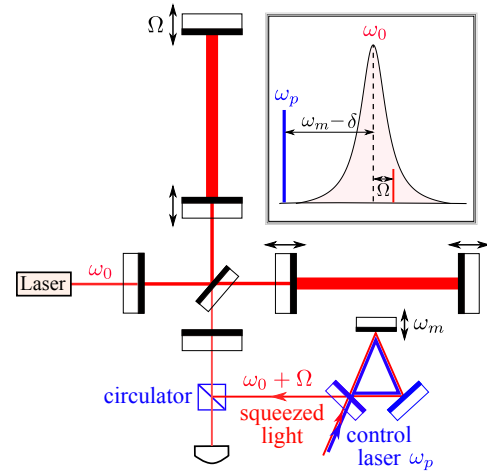


FIG. 1: (Color online) Schematic showing the configuration for achieving frequency-dependent squeezing at low frequencies by filtering frequency-independent squeezed light through a filter cavity of which the bandwidth is narrowed via optomechanical interaction.

relation for the sideband field at $\omega_0 + \Omega$:

$$\hat{a}_{\text{out}}(\Omega) \approx \frac{\Omega - \delta - i\gamma_{\text{opt}}}{\Omega - \delta + i\gamma_{\text{opt}}} \hat{a}_{\text{in}}(\Omega) + \hat{n}_{\text{th}}(\Omega), \quad (1)$$

where γ_{opt} is defined as:

$$\gamma_{\text{opt}} = \frac{\hbar \bar{G}_0^2}{2m\omega_m\gamma} \quad (2)$$

with \bar{G}_0 being the optomechanical coupling constant related to the pumping power of the control laser and m being the mass of the mechanical oscillator. The first term in Eq.1 gives the input-output relation of a standard optical cavity with the original cavity bandwidth γ replaced by γ_{opt} , which can be significantly smaller than γ , depending on the pumping power of the control laser and the mechanical oscillator that we use.

The second term \hat{n}_{th} arises from the thermal fluctuation of the mechanical oscillator. It is uncorrelated with the input optical field \hat{a}_{in} and therefore has a similar effect to that of the optical loss, decreasing the coherence of the squeezed light. In order for its effect to be small, we require

$$\frac{8k_B T}{Q_m} < \hbar\gamma_{\text{opt}} \quad (3)$$

with Q_m the mechanical quality factor and T the environmental temperature. Given the fact that the desired effective cavity bandwidth is $\gamma_{\text{opt}} \approx 2\pi \times 100 \text{ s}^{-1}$, we have

$$\frac{T}{Q_m} < 6.0 \times 10^{-10} \text{ K}. \quad (4)$$

This is quite challenging to achieve even with low-loss materials at cryogenic temperature. A possible near-term solution is using the idea of optical dilution, in which the restoring force of the mechanical oscillator is mostly provided by the lossless optical field instead of the elasticity. This can be realized by using an optical trap proposed by Chang *et al.* [8] and Ni *et al.* [9], or more recently, by Korth *et al.* [10]. The idea is to store the potential energy U_{tot} mostly in the lossless optical field instead of the lossy mechanical internal stress, i.e., $U_{\text{tot}} = U_{\text{opt}} + U_{\text{mech}}$ with $U_{\text{opt}} \gg U_{\text{mech}}$, and the ratio between these two gives the dilution factor. This can significantly boost the mechanical quality factor. As we will show later, an effective quality factor above 10^9 can be realized with achievable parameters [cf. Table I in the paper].

Optomechanical dynamics.—Here we provide the details for Eq. (1) by analysing dynamics of the optomechanically coupled optical cavity from the standard linearized Hamiltonian [11]:

$$\begin{aligned} \hat{\mathcal{H}} = & \hbar\omega_0 \hat{a}^\dagger \hat{a} + \frac{\hat{p}^2}{2m} + \frac{1}{2}m\omega_m^2 \hat{x}^2 + \hbar\bar{G}_0 \hat{x}(\hat{a}^\dagger + \hat{a}) \\ & + i\hbar\sqrt{2\gamma}(\hat{a}^\dagger \hat{a}_{\text{in}} e^{-i\omega_p t} - \hat{a} \hat{a}_{\text{in}}^\dagger e^{i\omega_p t}). \end{aligned} \quad (5)$$

Here ω_0 and ω_m are the resonant frequencies for the cavity and mechanical oscillator, respectively; the coupling constant is $\bar{G}_0 = (P\gamma\omega_0/[\hbar(\Delta^2 + \gamma^2)L_c^2])^{1/2}$ with L_c the cavity length and P the input laser power of the control field and detuning $\Delta \equiv \omega_0 - \omega_p$; \hat{a}_{in} is the annihilation operator for the input optical field (the squeezed light in our case). In the rotating frame at frequency ω_p of the control laser, the linear equations of motion for the perturbed part—variation around the steady-state amplitude—reads:

$$m(\ddot{\hat{x}} + \gamma_m \dot{\hat{x}} + \omega_m^2 \hat{x}) = -\hbar\bar{G}_0(\hat{a} + \hat{a}^\dagger) + \hat{F}_{\text{th}}, \quad (6)$$

$$\dot{\hat{a}} + (\gamma + i\Delta)\hat{a} = -i\bar{G}_0 \hat{x} + \sqrt{2\gamma} \hat{a}_{\text{in}}, \quad (7)$$

where we have included the damping term $m\gamma_m \dot{\hat{x}}$ for the mechanical oscillator and the associated thermal fluctuation force \hat{F}_{th} . These equations of motion can be solved in the frequency domain. For the mechanical displacement, we get

$$\hat{x}(\omega) = \chi_m^{-1}(\omega) \left\{ \hbar\bar{G}_0[\hat{a}(\omega) + \hat{a}^\dagger(-\omega)] + \hat{F}_{\text{th}}(\omega) \right\}, \quad (8)$$

$$\hat{a}(\omega) = \chi_c^{-1}(\omega) [-i\bar{G}_0 \hat{x}(\omega) + \sqrt{2\gamma} \hat{a}_{\text{in}}(\omega)]. \quad (9)$$

Here $\chi_m \equiv -m(\omega^2 - \omega_m^2 + i\gamma_m\omega)$ and $\chi_c \equiv \gamma - i(\omega - \Delta)$ are the inverse of the mechanical and the cavity response function, respectively; ω is the sideband frequency with respect to the control laser frequency ω_p .

Relevant parameter regime.— Here we narrow down to the one that is relevant to our proposed scheme. In particular, we consider the case where $\Delta = \omega_m - \delta$ with $\omega_m \gg \delta \approx 2\pi \times 100 \text{ s}^{-1}$. Additionally, we limit ourselves to the resolved-sideband regime with the mechanical resonant frequency larger than the cavity bandwidth, i.e., $\omega_m > \gamma$. Correspondingly, the lower sideband of the cavity mode $\hat{a}(-\omega)$ in Eq. (8) is negligibly small and can be ignored (we will analyze the effect of this approximation later). We therefore obtain [cf. Eqs. (8) and (9)]:

$$\hat{a}(\omega) \approx \frac{\sqrt{2\gamma} \hat{a}_{\text{in}}(\omega) - i\bar{G}_0 \chi_m^{-1}(\omega) \hat{F}_{\text{th}}(\omega)}{\chi_c(\omega) + i\hbar\bar{G}_0^2 \chi_m^{-1}(\omega)}. \quad (10)$$

Note that we are interested in the sideband frequencies Ω (the signal frequency) around ω_0 . We can therefore rewrite the above expression in terms of Ω by using the equality $\omega = \Delta + \Omega$ [cf. the inset of Fig.(1)]. In addition, since $\Omega \approx \delta \ll \omega_m$, we can approximate χ_m and χ_c as:

$$\chi_m \approx -2m\omega_m(\Omega - \delta + i\gamma_m), \quad \chi_c \approx \gamma. \quad (11)$$

This gives rises to

$$\hat{a}(\Omega) \approx \frac{\sqrt{2\gamma}(\Omega - \delta + i\gamma_m)\hat{a}_{\text{in}}(\Omega) + i\gamma_{\text{opt}}\hat{F}_{\text{th}}(\Omega)/(\hbar\bar{G}_0)}{\Omega - \delta + i\gamma_m - i\gamma_{\text{opt}}}. \quad (12)$$

From the standard input-output relation, the output field of the cavity \hat{a}_{out} is related to the cavity mode \hat{a} by $\hat{a}_{\text{out}} =$

TABLE I: Sample parameters for the cavity and the laser fields for the scheme shown in Fig.2

Parameters	Value	Description
L	0.4m	cavity length
T_f	100ppm	front mirror transmission
T_e	10ppm	end mirror transmission
T_s	10^4 ppm	intra-cavity mirror transmission
P_{trap}	1.25mW	trapping beam input power
Δ_t	75MHz	frequency difference between the trapping beam and cavity resonance
m	550ng	bare mass of mechanical oscillator
ω_m	100s^{-1}	resonant frequency of mechanical oscillator
γ_m	$1 \times 10^{-6}\text{s}^{-1}$	bandwidth of mechanical oscillator
T	0.5K	environmental temperature
P_{control}	$30\mu\text{ W}$	control beam injection power

$-\hat{a}_{\text{in}} + \sqrt{2\gamma}\hat{a}$, which leads to

$$\hat{a}_{\text{out}}(\Omega) \approx \frac{\Omega - \delta + i\gamma_m - i\gamma_{\text{opt}}}{\Omega - \delta + i\gamma_m + i\gamma_{\text{opt}}} \hat{a}_{\text{in}}(\Omega) + \hat{n}_{\text{th}}(\Omega) \quad (13)$$

with the additional noise term \hat{n}_{th} defined as

$$\hat{n}_{\text{th}}(\Omega) = \frac{i\sqrt{2\gamma}\gamma_{\text{opt}}\hat{F}_{\text{th}}(\Omega)}{\hbar\bar{G}_0(\Omega - \delta + i\gamma_m - i\gamma_{\text{opt}})}. \quad (14)$$

For a high quality factor oscillator, $\gamma_{\text{opt}} \gg \gamma_m$. By ignoring γ_m , we recover the input-output relation shown in Eq. (1).

To maintain the coherence of squeezed light, the thermal noise term \hat{n}_{th} needs to have a fluctuation that is much smaller than the vacuum level, or equivalently, the quantum radiation pressure of the squeezed light needs to dominate over the thermal noise. Given the fact that in the high temperature limit, $\langle \hat{F}_{\text{th}}^\dagger(\Omega)\hat{F}_{\text{th}}(\Omega') \rangle = 4m\gamma_mk_BT\delta(\Omega - \Omega')$ (single-sided spectrum), the requirement on the noise spectrum for \hat{n}_{th} reads

$$S_{\text{th}}(\Omega) = \left(\frac{8k_BT}{\hbar\gamma_{\text{opt}}Q_m} \right) \frac{\gamma_{\text{opt}}^2}{(\Omega - \delta)^2 + \gamma_{\text{opt}}^2} < 1. \quad (15)$$

The effect of thermal noise is most prominent for $\Omega \sim \delta$, from which we obtain the condition shown in Eq. (3).

Effects of optical loss and finite cavity bandwidth.— Apart from the above-mentioned thermal noise, there are other decoherence effects that we have ignored in the previous discussion: (i) the optical loss, which will introduce uncorrelated vacuum noise, and also (ii) the finite cavity

bandwidth, which allows the lower sideband, ignored in the resolved-sideband limit, to play a non-negligible role. Their effects are similar to the above thermal force noise; therefore we can quantify their magnitude by converting their spectrum into the force noise spectrum. For the optical loss, the corresponding force spectrum reads

$$S_F^{\text{loss}} = \frac{2\hbar^2\bar{G}_0^2\gamma'}{\Omega^2 + (\gamma + \gamma')^2} \approx \frac{2\hbar^2\bar{G}_0^2\gamma'}{\gamma^2}, \quad (16)$$

where $\gamma' = c\epsilon/(4L_c)$ and ϵ is the magnitude of the optical loss (e.g., $\epsilon = 10^{-5}$ for 10ppm loss). Normalizing by the transfer function from force to \hat{a}_{out} [cf. Eq. (14)], the equivalent noise spectrum is given by

$$S_{\text{loss}}(\Omega) = \left(\frac{4\gamma'}{\gamma} \right) \frac{\gamma_{\text{opt}}^2}{(\Omega - \delta)^2 + \gamma_{\text{opt}}^2}. \quad (17)$$

Similarly, for the lower sideband, after normalizing by the transfer function, we have

$$S_{\text{lower}}(\Omega) \approx \left(\frac{\gamma}{\omega_m} \right)^2 \frac{\gamma_{\text{opt}}^2}{(\Omega - \delta)^2 + \gamma_{\text{opt}}^2}, \quad (18)$$

Therefore, in order for this scheme to work, in addition to the requirement shown in Eq. (3), we require

$$\frac{4\gamma'}{\gamma} \ll 1, \quad \left(\frac{\gamma}{\omega_m} \right)^2 \ll 1, \quad (19)$$

which means that a small optical loss and resolved sideband limit are necessary.

Possible experimental scheme.—As we have mentioned earlier, the most significant issue is the thermal noise as shown by the condition in Eq. (4), which puts a strin-

gent requirement on the mechanical property and also the environment temperature. This problem can possibly be solved by using optical dilution proposed and exper-

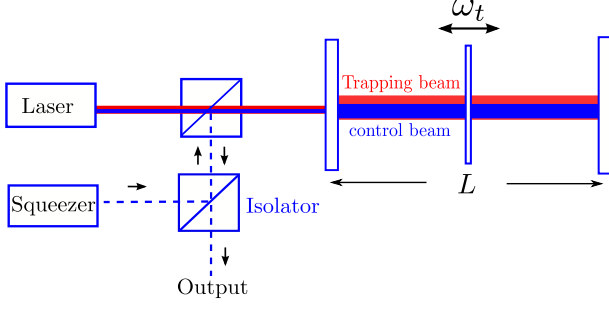


FIG. 2: Schematics for a possible experimental scheme that incorporates the optical dilution idea proposed in Ref. [10]. Here an auxiliary cavity (right side) is attached to the filter cavity (left side) to create a strong double optical spring for the mechanical oscillator, which can dilute the mechanical damping and enhance the mechanical quality factor.

imentally demonstrated by Corbitt et.al [7]. Basically, optomechanical interaction can modify the dynamics of the mechanical degrees of freedom, increase the mechanical resonant frequency, thereby increasing the mechanical Q -factor.

Here, we consider the optical dilution idea based on the experimental setup proposed in [12]. This scheme is shown schematically in Fig.2.

A high-reflective vibrating mirror with transmissivity T_s is placed in the middle of a Fabry-Perot cavity whose front and end mirrors have transmissivity T_f and T_e , respectively. A laser beam is injected into the system for trapping the intra-cavity mirror thereby increasing this mirror's Q -factor. The trapping frequency is given by:

$$\omega_{\text{opt}}^2 = \frac{\hbar G_0^2 \bar{a}_t^2}{m \omega_s \gamma_f}. \quad (20)$$

Here $\bar{a}_t = \sqrt{P_{\text{trap}}/\hbar\omega_c}$ is the strength of the incoming trapping beam (P_{trap} and ω_c as the input power and frequency of the trapping beam respectively) and $\gamma_f = cT_f/2L_c$. Linear optomechanical interaction in the right subcavity creates the trapping rigidity. For details, see [13]. In this case, the mechanical Q -factor becomes $Q_m^{\text{eff}} = (\omega_m + \omega_{\text{opt}})/\gamma_m$.

However, there are several issues that must be addressed. The first one is the trapping beam will introduce an additional back-action noise to the optically-trapped mirror, which potentially will degrade the coherence of the squeezed light. Interestingly, we found that (detailed derivations are described in *Appendix*) this system will evade this back-action noise when the detuning Δ_t of the trapping beam is equal to 'sloshing frequency' $\omega_s = c\sqrt{T_s}/4L_c$ and the end mirror is perfectly reflective. The physics behind this back-action evasion effect can be described as the following (See Fig.A4 in *Appendix*): the optical field reflected by the trapped-mirror consists of the prompt reflection from the trapped-mirror plus the

leakage field of light circulating in the right-half cavity. Both of these two parts contain the displacement signal of the trapped mirror and will destructively cancel with each other. Destructive interference of the displacement signal is equivalent to zero linear back-action noise.

In reality there is no perfect reflective mirror, therefore, inevitably residual radiation pressure noise must exist, given by:

$$S_{\text{FF}}^{\text{res}} = 2\hbar^2 G_0^2 \frac{\bar{a}_t^2}{\omega_s^2} \frac{\gamma_e}{\gamma_f} + O\left(\left(\frac{\gamma_e}{\gamma_f}\right)^2\right), \quad (21)$$

with $\gamma_e = cT_e/2L$. Decreasing the end mirror transmissivity (which can be as small as 1ppm in some cases [15]) can reduce the radiation pressure noise to satisfy the requirement of the OMIT filter cavity experiment. This noise is equivalent to a thermal bath with effective temperature $T_{\text{eff}} = S_{\text{FF}}^{\text{res}}/4m\gamma_m k_B$. Crediting the influence of the residual radiation pressure noise and optical rigidity, we require that $(T + T_{\text{eff}})/Q_m^{\text{eff}} < 6.0 \times 10^{-10} \text{K}$ instead of (4).

In addition to the back-action noise, the velocity and acceleration response of the trapped mirror may affect the stability of the system. Analysis in *Appendix* shows that for the special parameter combination ($\Delta_t = \omega_s$, $\gamma_e/\gamma_f \ll 1$) one can have a small negative damping factor which will be compensated by the control beam which cools the trapped mirror. Moreover, acceleration response of the trapped mirror is also discussed in *Appendix*, which shows that the related negative inertia effect will not create instability near this specific parameter region.

Lastly, the heating of the trapped mirror by high intra-cavity power laser field constraints the choice of the parameters of trapped mirror since this heating effect will introduce more thermal noise, which makes this experiment even more challenging. In the following section, we will discuss this point by using our sample parameters.

A sample set of parameters.—To illustrate the requirements for experimentally realizing the proposed scheme, we give a sample set of parameters in Tab.I. Under this set of sample parameters, the filter cavity bandwidth changes from its original value of 50KHz to $\gamma_{\text{opt}} \sim 100\text{Hz}$ (see Tab.II), narrowed by a factor of 500. The double optical spring created by the auxiliary cavity shifts the mechanical frequency from 100Hz up to $\omega_m^{\text{eff}} \sim 185\text{kHz}$, resulting in an enhancement of the mechanical quality factor by almost one thousand. Including the effect of residual radiation pressure noise and the temperature increase due to the absorption of trapping beam, this gives $T_{\text{total}}/Q_m^{\text{eff}} = 1.4 \times 10^{-10}$ which satisfies the condition shown in Eq. (4) (The T_{total} here consists of environmental (0.5K), heating temperature ($\approx 20\text{K}$ [16]) and T_{eff}). The sample parameters for the cavity configurations and the light beam are listed in Tab.I. Notice that the power given here are all external pumping power. The mechanical dynamics are modified by

TABLE II: Derived Parameters for trapped mirror dynamics

Parameters	Value	Description
ω_{opt}	$1.85 \times 10^5 \text{s}^{-1}$	optical spring frequency Eq.(A.8)
Γ	-0.18s^{-1}	optical (anti-)damping rate by trapping beam Eq.(A.9)
m_{opt}	$3.4 \times 10^{-3} \text{ng}$	negative inertia by trapping beam Eq.(A.10)
T_{eff}	6.2K	effective temperature of the residue radiation pressure noise Eq.(A.11)(A.12)
Q_m^{eff}	1.8×10^{11}	mechanical Q factor of the trapped mirror.
γ_{opt}	$2\pi \times 53 \text{s}^{-1}$	effective optomechanical cavity bandwidth

the opto-mechanical interaction, and the new effective parameters of the vibrating mirror are summarised in Tab.II. Comparing the magnitude of T_{eff} , m_{opt} , and Γ , to the corresponding quantities in Tab.I, we can see that the residual radiation pressure noise and the velocity and acceleration response of the trapped mirror do not pose a significant problem with parameters listed in Table I. The trapped mirror needs to be a high reflectivity mirror with low mass, low optical and mechanical losses, which could

be a cantilever [17] or even a mirror suspended in pendulum [18]. Some of the parameters there are challenging and may not be achievable in short term.

In general, we would like to emphasise that although using OMIT effect to build a optomechanical filter cavity is itself an interesting idea, the experiment, particularly considering the requirements on optical absorption/physical cooling power noted earlier, is extremely challenging.

Conclusion.—We have considered the use of optomechanical interaction to narrow the bandwidth of a filter cavity for frequency-dependent squeezing in future advanced gravitational-wave detectors. This has the appealing prospect of achieving low-frequency filtering in a compact tabletop setup and with tunable bandwidth. Due to susceptibility to thermal decoherence, its feasibility is conditional on advancements in low-loss mechanics and optics. Although this proposal is difficult to achieve with current technology, it is worth considering for future filter cavity designs.

Acknowledgements.—We thank Huan Yang, David McClelland, Farid Khalili, Li Ju and Jiayi Qin for fruitful discussions. Y.M., S.D., C.Z. have been supported by the Western Australia Centers of Excellence program, and by the Australian Research Council; W.Z.K. is supported by NSF Grant PHY-0757058; H.M. and Y.C. are supported by NSF Grants PHY-1068881 and CAREER Grant PHY-0956189.

* Electronic address: myqphy@gmail.com

† Electronic address: chunnong.zhao@uwa.edu.au

‡ Electronic address: haixing@caltech.edu

- [1] B. P. Abbott, R. Abbott, R. Adhikari, P. Ajith, B. Allen, G. Allen, R. S. Amin, S. B. Anderson, W. G. Anderson, M. A. Arain, et al., Reports on Progress in Physics 72, 076901 (2009), URL <http://stacks.iop.org/0034-4885/72/i=7/a=076901>.
- [2] H. J. Kimble, Y. Levin, A. B. Matsko, K. S. Thorne, and S. P. Vyatchanin, Phys. Rev. D 65, 022002 (2001).

- [3] M. Evans, L. Barsotti, P. Kwee, J. Harms and H. Miao Phys. Rev. D 88, 022002 (2013), URL <http://prd.aps.org/pdf/PRD/v88/i2/e022002>
- [4] E. E. Mikhailov, K. Goda, T. Corbitt, and N. Mavalvala, Phys. Rev. A 73, 053810 (2006), URL <http://link.aps.org/doi/10.1103/PhysRevA.73.053810>.
- [5] S. Weis, R. Riviere, S. Deléglise, E. Gavartin, O. Arcizet, A. Schliesser, and T. J. Kippenberg, Science 330, 1520 (2010), URL <http://www.sciencemag.org/content/330/6010/1520.abstract>.
- [6] J. D. Teufel, D. Li, M. S. Allman, K. Cicak, A. J. Sirois, J. D. Whittaker, and R. W. Simmonds, Nature 471, 204(2011), ISSN 0028-0836, URL <http://dx.doi.org/10.1038/nature09898>.
- [7] T. Corbitt, Y. Chen, E. Innerhofer, H. Muller-Ebhardt, D. Ottaway, H. Rehbein, D. Sigg, S. Whitcomb, C. Wipf and N. Mavalvala URL <http://prl.aps.org/pdf/PRL/v98/i15/e150802>
- [8] D. E. Chang, K.-K. Ni, O. Painter, and H. J. Kimble, New Journal of Physics 14, 045002 (2012), URL <http://stacks.iop.org/1367-2630/14/i=4/a=045002>.
- [9] K.-K. Ni, R. Norte, D. J. Wilson, J. D. Hood, D. E. Chang, O. Painter, and H. J. Kimble, Phys. Rev. Lett. 108, 214302 (2012), URL <http://link.aps.org/doi/10.1103/PhysRevLett.108.214302>.
- [10] W. Z. Korth, H. Miao, T. Corbitt, G. D. Cole, Y. Chen, and R. X. Adhikari, arXiv:1210.0309 [quant-ph] (2012).
- [11] F. Marquardt, J. P. Chen, A. A. Clerk, and S. M. Girvin, Phys. Rev. Lett. 99, 093902 (2007), URL <http://link.aps.org/doi/10.1103/PhysRevLett.99.093902>.
- [12] A. M. Jayich, J. C. Sankey, B. M. Zwickl, C. Yang, J. D. Thompson, S. M. Girvin, A. A. Clerk, F. Marquardt, and J. G. E. Harris, New J. Phys. 10, 095008 (2008), URL <http://iopscience.iop.org/1367-2630/10/9/095008>.
- [13] H. Miao, Y. Ma, H. Yang, and Y. Chen, in preparation (2013).

- [14] H. Miao, S. Danilishin, T. Corbitt, and Y. Chen, Phys. Rev. Lett. 103, 100402 (2009), URL <http://link.aps.org/doi/10.1103/PhysRevLett.103.100402>.
- [15] G. Rempe, R. J. Thompson, H. J. Kimble and R. Lalezari Vol.17, No.5 363 (1992), URL <http://www.opticsinfobase.org/ol/abstract.cfm?uri=ol-17-5-363>
- [16] S. Danilishin, private note.
- [17] G. D. Cole, Proceedings of the SPIE, Volume 8458, article id. 845807, 11 pp. (2012). URL <http://proceedings.spiedigitallibrary.org/proceeding.aspx?articleid=1367575#>
- [18] G. Cagnoli, L. Gammaitoni, J. Hough, J. Kovalik, S. McIntosh, M. Punturo and S. Rowan. Phys. Rev. Lett, 85, 2442, (2000), URL http://prl.aps.org/abstract/PRL/v85/i12/p2442_1

Appendix

In this Appendix, we will show some additional details and derivations for the dynamics of the optomechanical dynamics of the scheme of Fig.A.3. Our notation here is nearly identical to that in [14]. We also give a summary of the parameters of our system in Tab.I and Tab.II.

Formulating the problem

The Hamiltonian of the system can be written as:

$$H = \hbar\omega_c(\hat{a}^\dagger\hat{a} + \hat{b}^\dagger\hat{b}) + \frac{\hat{p}^2}{2m} + \frac{1}{2}m\omega_m^2\hat{x}^2 + \hbar\omega_s(\hat{a}^\dagger\hat{b} + \hat{a}\hat{b}^\dagger) + \hbar G_0\hat{x}(\hat{a}^\dagger\hat{a} - \hat{b}^\dagger\hat{b}) + H_{ext}^{opt} + H_{ext}^m \quad (\text{A.1})$$

Here, \hat{a}, \hat{b} are annihilation operators for cavity modes in left and right sub-cavity (with resonant frequency ω_c) respectively. \hat{x}, \hat{p} are the position and momentum operators of the vibrating mirror. ω_s is the coupling constant for \hat{a} and \hat{b} . $H_{ext}^{opt} = i\hbar\sqrt{2\gamma_f}(\hat{a}^\dagger\hat{a}_{in} - \text{h.c.}) + i\hbar\sqrt{2\gamma_e}(\hat{b}^\dagger\hat{b}_{in} - \text{h.c.})$ and H_{ext}^m correspond to the coupling of the system to the environment.

The Heisenberg equation of motion can be derived as:

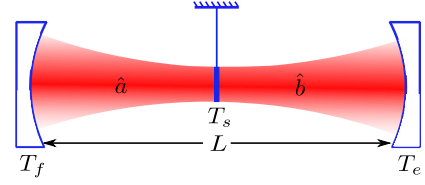


FIG. A.3: Basic configuration of the proposed scheme: a vibrating mirror trapped in an Fabry-Perot cavity.

$$\dot{\hat{a}} = i\omega_s\hat{a} - \gamma_f\hat{a} - i\omega_s\hat{b} - iG_0\hat{x}\hat{a} + \sqrt{2\gamma_f}\hat{a}_{in} \quad (\text{A.2a})$$

$$\dot{\hat{b}} = i\omega_s\hat{b} - \gamma_e\hat{b} - i\omega_s\hat{a} + iG_0\hat{x}\hat{b} + \sqrt{2\gamma_e}\hat{b}_{in} \quad (\text{A.2b})$$

$$\dot{\hat{p}} = -m\omega_m^2\hat{x} - \gamma_m\hat{p} - G_0(\hat{a}^\dagger\hat{a} - \hat{b}^\dagger\hat{b}) + F_{th} \quad (\text{A.2c})$$

$$\dot{\hat{x}} = \hat{p}/m \quad (\text{A.2d})$$

Here, $\gamma_f = cT_f/2L$ and $\gamma_e = cT_e/2L$, T_f and T_e are the transmissivity of the front mirror and the end mirror. Suppose we pump the cavity field by injecting a laser field through the front mirror (*single-side pumping*), then $\hat{b}_{in} = 0$. These equations can be solved perturbatively. The zeroth order terms give us the classical amplitude of the intra-cavity mode in both sub-cavities and the first order terms carries the information of mirror vibration along with quantum noise due to the non-zero transmissivity of cavity end mirror.

In the frequency domain and working in the rotating frame of the frequency of the pumping fields, we have the steady field in the two sub-cavities:

$$\bar{a} = \frac{(i\Delta_t - \gamma_e)\sqrt{2\gamma_f}\bar{a}_{in}}{\Delta_t^2 - \omega_s^2 - \gamma_f\gamma_e + i\Delta_t(\gamma_f + \gamma_e)} \quad (\text{A.3a})$$

$$\bar{b} = \frac{i\sqrt{2\gamma_f}\omega_s\bar{a}_{in}}{\Delta_t^2 - \omega_s^2 - \gamma_f\gamma_e + i\Delta_t(\gamma_f + \gamma_e)}, \quad (\text{A.3b})$$

where Δ_t is the detuning of the trapping laser field with respect to the resonant frequency of half-cavity. The fluctuation field consists of mechanical modulation and quantum fluctuation as:

$$\hat{a}(\omega) = \frac{-G_b\omega_s\hat{x} + i\omega_s\sqrt{2\gamma_b}\hat{b}_{in} + [i(\omega + \Delta_t) - \gamma_b][-iG_a\hat{x} + \sqrt{2\gamma_a}\hat{a}_{in}]}{(\omega + \Delta_t)^2 - \omega_s^2 - \gamma_e\gamma_f + i(\omega + \Delta_t)(\gamma_f + \gamma_e)} \quad (\text{A.4a})$$

$$\hat{b}(\omega) = \frac{G_a\omega_s\hat{x} + i\sqrt{2\gamma_a}\omega_s\hat{a}_{in} + [i(\omega + \Delta_t) - \gamma_a](iG_b\hat{x} + \sqrt{2\gamma_b}\hat{b}_{in})}{(\omega + \Delta_t)^2 - \omega_s^2 - \gamma_e\gamma_f + i(\omega + \Delta_t)(\gamma_f + \gamma_e)} \quad (\text{A.4b})$$

The radiation pressure force acting on the trapped mirror

is given by

$$\hat{F}_{rad}(\omega) = \hbar[G_a^*\hat{a}(\omega) - G_b^*\hat{b}(\omega)] + \text{h.c.} \quad (\text{A.5})$$

which can be split into two parts:

$$\hat{F}_{\text{rad}}(\omega) = -K_{\text{opt}}(\omega)\hat{x}(\omega) + \hat{F}_{\text{BA}}(\omega) \quad (\text{A.6})$$

The first and second term represent the pondermotive modification of the mechanical dynamics and the back-action quantum radiation pressure noise respectively. The $K_{\text{opt}}(\omega)$ here is the optomechanical rigidity which can be expanded in terms of ω if the typical frequency of mechanical motion is smaller than the other frequency scale in the trapping system:

$$-K_{\text{opt}}(\omega) \approx -K_{\text{opt}}(0) - \frac{\partial K_{\text{opt}}}{\partial \omega} \omega - \frac{1}{2} \frac{\partial^2 K_{\text{opt}}}{\partial \omega^2} \omega^2 \quad (\text{A.7})$$

The first term in (A.7) gives the trapping frequency and the second and third term give the velocity and acceleration response of the trapped mirror which are optical (anti-)damping Γ and optomechanical inertia m_{opt} , respectively.

Substituting (A.3) and (A.4) into (A.5) and taking the expansion with respect to detection frequency ω , we can get the analytical expression of the optical rigidity and radiation pressure noise. However, they are too cumbersome to show. In the following, we show approximate results in the parameter region of $\Delta_t \sim \omega_s$ and $\gamma_e \ll \gamma_f$.

Dynamics and back-action

The optical spring frequency is given by:

$$\omega_{\text{opt}}^2 = \frac{\hbar G_0^2 \bar{a}_t^2}{m \omega_s \gamma_f} + o(\epsilon) \quad (\text{A.8})$$

Here, for consistency with the main text, we use \bar{a}_t to represent the external pumping beam amplitude rather than \bar{a}_{in} . Moreover, \bar{a}_t is related to the trapping beam power P_{trap} through $\bar{a}_t = \sqrt{P_{\text{trap}}/\hbar\omega_0}$. The $o(\epsilon)$ here describes all the high order terms with $\epsilon \sim (\Delta_t - \omega_s)/\omega_s, \gamma_e/\gamma_f$. Notice that this optical spring can be treated effectively as a quadratic trap of the vibrating mirror on the anti-node of our trapping beam as shown in [14]

The optical (anti-)damping factor Γ is given by extending $K_{\text{opt}}(\omega)$ to 1st order of ω :

$$\Gamma = \frac{16\hbar G_0^2 \bar{a}_t^2}{m \gamma_f^2 \omega_s} \left(\frac{\Delta_t - \omega_s}{\omega_s} \right) - \frac{8\hbar G_0^2 \bar{a}_t^2}{m \omega_s^3} \left(\frac{\gamma_e}{\gamma_f} \right) + o(\epsilon^2) \quad (\text{A.9})$$

It is clear from this formula that in the ideal case when $\Delta_t = \omega_s$ and $\gamma_e = 0$, the optical damping is completely cancelled. Therefore by carefully choosing the system parameters, we can achieve a small positive damping when the end mirror is not perfectly reflective.

The optomechanical inertia, i.e. acceleration response is given by extending $K_{\text{opt}}(\omega)$ to 2nd order of ω , the main contribution is at zeroth order of ϵ :

$$m_{\text{opt}} = -\frac{\hbar G_0^2 \bar{a}_t^2}{\gamma_f \omega_s^3} + o(\epsilon) \quad (\text{A.10})$$

which is extremely small as we have shown in the main text.

Finally, the back-action radiation pressure force noise spectrum is given by:

$$S_{\text{FF}}^{\text{rad}} = \frac{2\hbar^2 G_0^2 \bar{a}_t^2}{\omega_s^2} \frac{\gamma_e}{\gamma_f} + o(\epsilon^2) \quad (\text{A.11})$$

Notice that the back-action force spectrum is zero when the end mirror is perfectly reflective ($\gamma_e = 0$). This residual radiation pressure noise is equivalent to a effective thermal bath with temperature:

$$T_{\text{eff}} = \frac{S_{\text{FF}}^{\text{rad}}}{4m\gamma_m k_B} \quad (\text{A.12})$$

The physical explanation of this back-action evasion phenomenon is shown in Fig.A.4. The part of the outgoing fields which contains the displacement signal can be written as (*suppose the end mirror is perfectly reflective*):

$$\hat{a}_{\text{out}}^m = -2iG_0 \bar{a}_{\text{in}} \hat{x} + 2i \frac{G_0 \bar{a}_{\text{in}} \omega_s^2}{\Delta_t^2} \hat{x} \quad (\text{A.13})$$

The first term on the right hand-side is the field directly reflected from the trapped mirror while the second term is the field transmitted out of the cavity. We can see that they cancel when $\Delta_t = \omega_s$. Therefore in this case the output field does not contain the x -information.

Here, given the parameters listed in Tab.I, we use (A.8)-(A.11) to calculate the modification of the mechanical dynamics by the trapping beam, and list the effective parameters in Tab.II. We can see that velocity response is a mechanical damping factor Γ which will not cause instability and is too small to affect the OMIT effective cavity bandwidth γ_{opt} . The negative inertia m_{opt} is also too small to be comparable to the mass of the mechanical oscillator. Most importantly, the requirement $(T + T_{\text{eff}})/Q_{\text{eff}}^m$ is satisfied.

OMIT effect

In this configuration, the system has two optical resonant frequencies at $\omega_0 + \omega_s$ and $\omega_0 - \omega_s$, corresponding to two eigenmodes $(\hat{a} + \hat{b})/\sqrt{2}$ and $(\hat{a} - \hat{b})/\sqrt{2}i$, respectively.

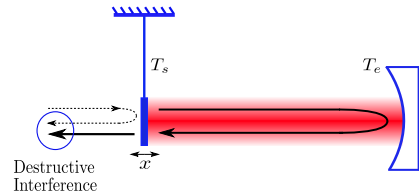


FIG. A.4: Back-action evasion: destructive interference between the field directly reflected from the oscillating mirror and the field transmitted out of the cavity.

If we pump the $\omega_0 + \omega_s$ mode, we will get an optical trap potential for the vibrating mirror as we have shown in the previous subsection; further more, as was shown in [14], the vibrating mirror can be effectively treated as being placed at the anti-node of the pump field. However, if we pump the other mode, we will get a negative

rigidity term. Nevertheless, this channel can be used for the OMIT experiment. The scheme is to inject the signal field near the resonance of $\omega_0 - \omega_s$ and the control field at $\omega_0 - \omega_s - \omega_m$. Since the control field is much weaker than the trapping field, the negative rigidity created by the control field is negligible.